Reconstructing past sea surface temperatures near the Iceland-Faroe Ridge using alkenone paleothermometry ($U^{k'}_{37}$)

By:

Stefanie Mellon

in

B.Sc. Honours Co-op Environmental Science, Dalhousie University

Supervisor: Dr. Markus Kienast, Professor of Oceanography, Dalhousie University

markus.kienast@dal.ca

April 3, 2015

Table of Contents

1.0 Acknowledgements

I would like to thank my supervisor, Dr. Markus Kienast, for his continuous support throughout the entire process of writing this honours thesis. I greatly appreciate the guidance provided by our Honours class instructor, Dr. Tarah Wright. I would like to thank Dr. Dirk Nürnberg and Maryam Mirzaloo for hosting me at GEOMAR Helmholtz Centre for Ocean Research Kiel, and for providing sample material and ancilliary data. I also thank Claire Normandeau for her help with laboratory work. And lastly, I would like to acknowledge TOSST Transatlantic Research School and NSERC for funding my summer research, in both Halifax, Canada and Kiel, Germany.

2.0 List of Abbreviations

LGM- Last Glacial Maximum
LSW- Labrador Slope Water
MOC- Meridional Overturning Circulation
NAC- North Atlantic Current
NAO- North Atlantic Oscillation
SST- Sea Surface Temperature

3.0 Abstract

Understanding the ocean and its past behaviour is important because it gives insight into rates and amplitudes of global change. This thesis uses a paleoceanographic technique (*Simplified Ketone Unsaturation Index* ($U^{k'}_{37}$)) that reconstructs sea surface temperatures (SST) of the past ocean in deep-sea sediment cores. SST is an important parameter because it is the temperature of the interface between oceanic and atmospheric heat reservoirs. The study site is located southeast of Iceland, which is of particular interest to oceanographers because it is a key region of deep-water formation. These data can be used to test the reliability of general circulation models (GCM). If GCMs can accurately simulate conditions of the past, then we can have more confidence in the models' predictions of future climate change.

Results of the study show two warm periods in the past that were both warmer than present day SSTs, and that the amplitude between warm and cold periods was 9 ±1.5°C. The exact age of the observed trends cannot be determined due to a lack of radiocarbon dating, therefore three potential age models are discussed in this thesis, based on lightness data of the core and the Northern Greenland Ice Core Project $\delta^{18}O$ record. Assuming that these age models are correct, we can conclude that the late Holocene (present day) was cooler than the early Holocene (11,700 years BP), and that the Last Glacial Maximum was warmer than present day SST values, based on $U^{k'}_{37}$ paleothermometry. The causes and implications of these findings will be discussed in the context of the literature. It is suggested that further research take place using another proxy measure and more sediment cores in order to better illustrate the past climate of this region.

4.0 Introduction

Paleoceanography is the study of the geologic history of the ocean in terms of its chemistry, biology, climate, and circulation patterns. Scientists use chemical indicators deposited in deep-sea sediments, called proxies, to reconstruct these ocean characteristics through time, often going back hundreds of thousands of years. We want to be able to use these proxy measures to reconstruct past climates so that we can have a better understanding of major climate events. These data can also be used to test the reliability of general circulation models (GCM). If GCMs can accurately simulate conditions of the past, then we can have more confidence in the model's predictions for future climate change.

The northern North Atlantic Ocean is of particular interest to paleoceanographers because it is a key region of deep-water formation. Changes in the rate of deep-water formation can affect rates of global heat and nutrient transport throughout the world's ocean. It is important to identify the instances in Earth's history in which these changes have occurred so that we can determine the effect that changing heat transport has on the global climate. The sea surface is an informative indicator of the state of past climates because it is the interface between the atmospheric and oceanic heat reservoirs. Sea surface temperature (SST) is therefore a useful climate parameter of the past. A common method for reconstructing sea surface temperatures uses alkenone unsaturation ratios from sediment cores (Brassel et al., 1986). For my honours project, I have reconstructed past SSTs using alkenone paleothermometry in an area of the North Atlantic, southeast of Iceland.

4.1 Background Information

The use of alkenones as a reliable paleothermometer was first appreciated by Brassel et al. (1986). This study found that the relative proportions of long-chain alkenones in sediments could be used to infer temperatures of the euphotic zone in the past and present ocean. Alkenones are long-chain, unsaturated carbon molecules that are present in three forms: di-unsaturated ($C_{37:2}$), tri-unsaturated ($C_{37:3}$), and tetra-unsaturated ($C_{37:4}$). The degree of unsaturation is based on the number of double bonds in the carbon chain (Brassel et al., 1986). These alkenones are synthesized as a function of growth temperature in a certain class of haptophyte algae, called coccolithophores. After death, the algae sink and get deposited in marine sediments throughout the majority of the world's ocean. The globally most abundant species of coccolithophore is *Emiliania huxleyi*, shown in Figure 1.

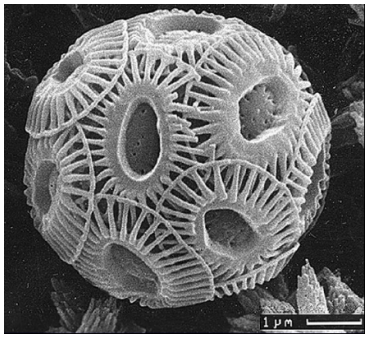

Figure 1. Image of *Emiliania huxleyi,* a species of coccolithophore that contains alkenones (Eglinton, 2007).

To quantify the temperature relationship with respect to the relative proportions of unsaturated alkenones, Brassel et al. (1986) proposed an index called U^k_{37}, given by Equation 1: $$U^k_{37} = \frac{C_{37:2} - C_{37:4}}{C_{37:2} + C_{37:3} + C_{37:4}}$$. Further research found that the tetra-unsaturated

alkenone is only produced in cold waters and does not correlate well with temperature (Sikes et. al 1996). The inclusion of $C_{37:4}$ in the U^{k}_{37} index increases the data scatter of the SST reconstruction. To account for this, a simplified index, called $U^{k'}_{37}$ was developed which excludes the $C_{37:4}$ term. The index is given by Equation 2:

$$U_{37}^{k\prime} = \frac{C_{37:2}}{C_{37:2} + C_{37:3}}$$

(Prahl and Wakeham, 1987). The temperature corresponding to this index can be inferred using a global core top calibration calculated by Müller et al. (1998), among others. This calibration is given by the following equation: $U^{k'}_{37}$= 0.033T+0.044, r^2= 0.958. Ambiguity still exists regarding habitat depth and seasonal distribution of *E. huxleyi* in the ocean (Conte et al., 2006). These variations and biases will be further discussed in Section 6.6 of this thesis.

My thesis is part of a cooperative project called "Iceland Hazards." This project aims to improve the knowledge of the spatial and temporal evolution of Icelandic Volcanism and its related hazards to human population and economy. The volcanoes of Iceland are not only hazardous for the local environments and economy, but also have impacts on regional and global scales due to high explosivity, wide ash dispersal, and abundant volcanic gas emissions (GEOMAR Report, 2013). These pose a major risk to air travel over the North Atlantic Ocean and to the health of people in northern Europe.

Scientists within this working group hope to develop a detailed tephrochronology of Iceland by studying marine sediment cores. Tephrochronology is a method of dating past geological events, based on discrete ash layers in the core (Lowe, 2011). Studying cores from this region also provides an opportunity to reconstruct past sea surface conditions of the seas surrounding Iceland.

4.2 Summary of Literature Review and Knowledge Gaps

The literature reviewed in Section 5.0 shows that, even though there have been multiple studies that attempt to reconstruct SST in the northern North Atlantic Ocean and Nordic Seas, there remain uncertainties regarding the state of past sea surface climates at high latitudes. Previous attempts to reconstruct SST have not focused on sediment cores from the Iceland Basin and Iceland-Faroe Ridge. Using alkenones to reconstruct SST dating back past the last ice age would be completely novel in this study region. There is also a lack of information about the effect that Icelandic volcanism has on the surrounding sea surface conditions. My thesis is aiming to address these knowledge gaps.

4.3 Objectives of Study

The objective of this study is to reconstruct the SSTs above the Iceland-Faroe Ridge in order to gain a better understanding of the climatic variations of this region. The study also aims to characterize mechanisms or events that may be causing variations in SST over time. Alkenone paleothermometry will be used as the proxy to reconstruct SST evolution of this region.

The research questions I will address in this thesis are:

- **What is the long-term (0-150,000 years B.P.) sea surface temperature variability in the downcore record from this region?**
    a. Do the results corroborate findings from previous climate reconstructions?
    b. Do the volcanoes of Iceland have an influence on the temperature signal of this region?

I hypothesize that the volcanoes of Iceland and solar insolation have a significant influence on the SST variability of this region.

To reconstruct past SSTs of the Iceland Basin and Iceland-Faroe Ridge region, I used the sampling and alkenone analysis techniques outlined in the Methods chapter (Section 6.0) of this thesis. The scope of this study is limited to the sampling area covered by the oceanographic research expedition P457, on the German *R/V Poseidon*. The locations of sampling stations from this cruise are presented in Figure 2. The core I used to reconstruct SSTs is named POS457-909-2-GC, located to the southeast of Iceland. Eleven core tops were also collected during this cruise to compare the $U^{k'}_{37}$ of this region to global calibrations.

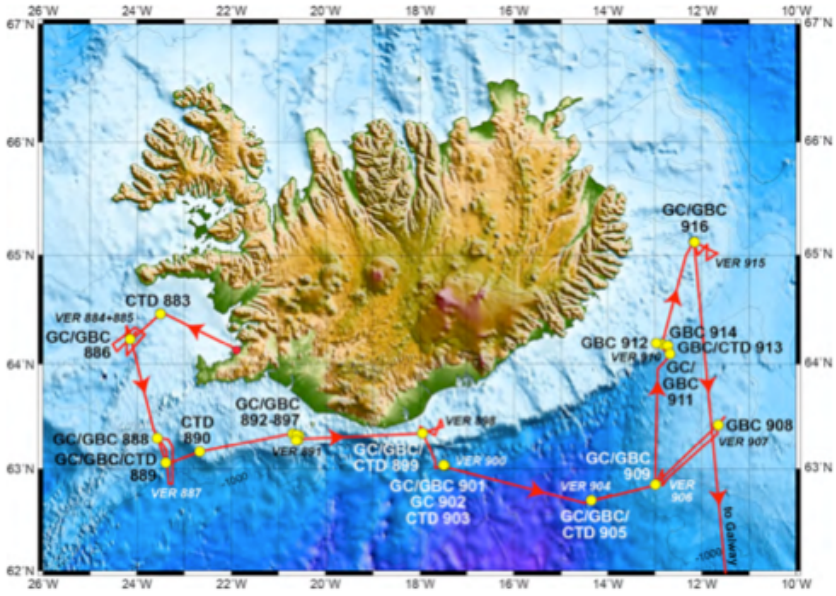

Figure 2: Route of the stations of cruise P457 around the South of Iceland. Abbreviations: VER- sediment echo sounding; GC- gravity corer; GBC- giant box corer; CTD- CTD + rosette water sampler (GEOMAR report, 2013).

5.0 Literature Review

5.1 Introduction

The purpose of this literature review is to demonstrate the need to conduct further research into the SST variability through geologic time in the Iceland Basin and Iceland Faroe-Ridge region. The knowledge of past SST values is useful for testing the performance of GCMs that predict the rate of future climate change. This particular region, southeast of Iceland, gives valuable information for simulating and predicting the microclimates of Northern Europe.

The northern North Atlantic is a critical region of the global thermohaline circulation because it is where cold, fresh, oxygen-rich waters sink to form deep waters that circulate the world's ocean. Understanding the mechanisms that influence the rate of deep-water formation can give insight into projected changes in global ocean circulation. Studying the SST estimates of this region will help scientists to quantify these mechanisms.

The Iceland Basin and Iceland-Faroe Ridge is also of significant interest because it is along the path of volcanic ash transport towards Europe. Volcanic eruptions pose a significant risk to human health in Northern Europe and to air travel over the North Atlantic Ocean (GEOMAR Report, 2013). Reconstructing SST estimates over the Iceland-Faroe Ridge would give insight into past ocean and atmospheric circulation changes, and whether the Icelandic volcanoes have an influence on the local climate.

This chapter will outline the understanding of the current state of the environment in the Iceland Basin and Iceland-Faroe Ridge including local temperature, salinity, dissolved oxygen, circulation, and bathymetry. The historical record of Icelandic

volcanism will be presented through terrestrial chronostratigraphy and historical accounts, as there is a lack of research on the marine record. This chapter will also present the previous attempts to reconstruct past sea surface temperatures of this region, focusing on findings from the last ice age up until the present epoch.

5.2 Circulation in the northern North Atlantic Ocean

The transport of large amounts of water and heat by means of global ocean currents is commonly known as the Thermohaline Circulation. In the North Atlantic, the density driven Meridional Overturning Circulation (MOC) influences this phenomenon. The MOC carries warm water north through two major water masses called the Gulf Stream and North Atlantic Current. A schematic of the MOC is given in Figure 3. At high latitudes off the coast of Canada, strong wintertime cooling forms intermediate-depth Labrador Sea Water (LSW) (Latif, 2006). This cold, salty water mass moves equatorward at depth through the Deep Western Boundary Current. This circulation is responsible for the relatively warm climate of the western North Atlantic (Latif, 2006).

The intensity of the MOC is influenced by the mid-depth density gradient between the subpolar Atlantic and South Atlantic Ocean (Hughes and Weaver, 2004). The density of subpolar Atlantic deep water is controlled by outflow waters from the Nordic Seas, as well as the density of overlying Labrador Sea Waters (LSW) (Latif et al., 2006). One of the controlling factors on the production of LSW is the variation in overlying atmospheric conditions, caused by the North Atlantic Oscillation (NAO). The NAO refers to the north-south oscillation of atmospheric mass with major axes centered near Iceland and in the subtropics, above the Azores (Hurrell, 2013). The changing heat fluxes resulting from the NAO have a significant impact on regional temperatures and

amount of precipitation over the North Atlantic Ocean. The changes in these climatic characteristics have an impact on rates of LSW formation, thus ultimately affecting the intensity of MOC.

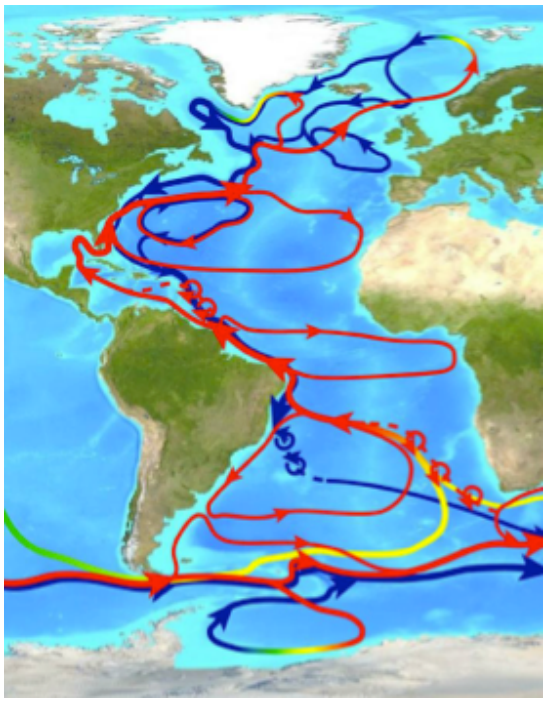

Figure 3. Schematic of the North Atlantic Meridional Overturning Circulation. The red lines represent the poleward moving surface waters and the blue lines represent the deep waters flowing southward from the region of formation (NOAA, 2013).

5.3 Oceanography of the Iceland Basin and Iceland-Faroe Ridge

5.3.1 Bathymetry

The bathymetry of the Iceland basin is documented in a review paper by Malmberg (2004). The boundaries of the basin include Reykjanes ridge in the west, Iceland in the north, and the Iceland-Faroe Ridge in the northeast. The southwest region is open to the Atlantic Ocean. These boundaries are evident in the bathymetric map of

the Iceland Basin, presented in Figure 4. The depth of the basin exceeds 2000 m in some regions and is less than 500 m at the peak of the Iceland-Faroe Ridge (Malmberg, 2004). The Iceland-Faroe Ridge is part of the Greenland-Iceland-Scotland Ridge that separates the North Atlantic Ocean from the Nordic Seas. It is a boundary between the relatively warm Northeastern Atlantic Water and the colder subarctic water masses (Malmberg, 2004).

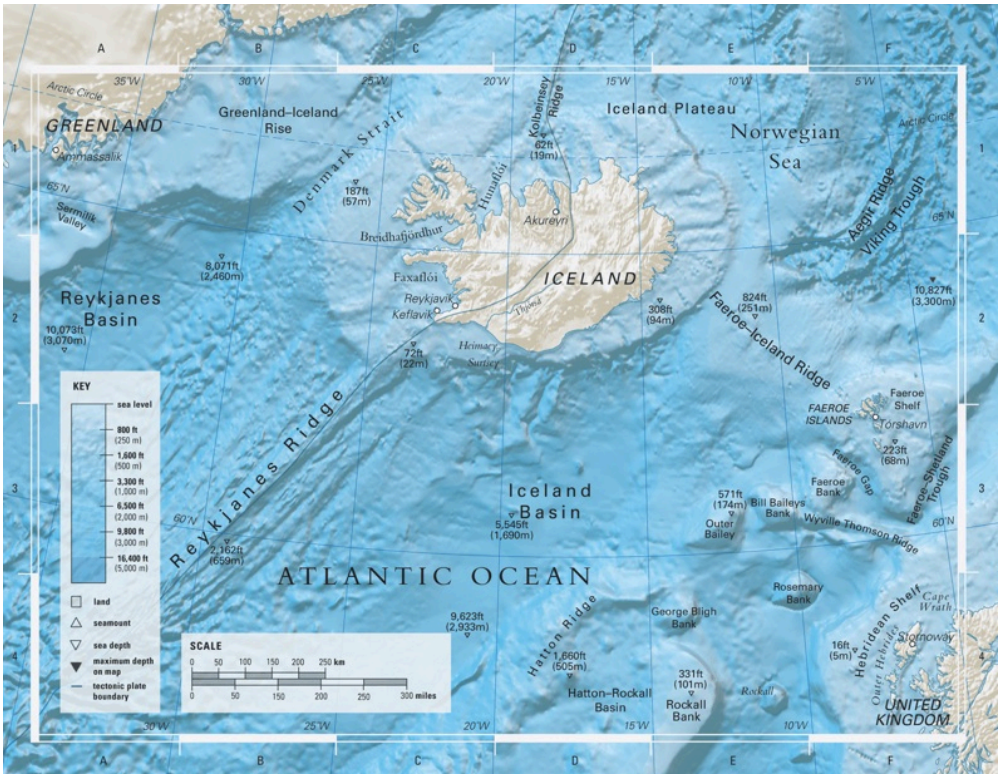

Figure 4: Bathymetric map of the Iceland Basin. The major geographic features of the region are labeled in black (Denmark Strait, n.d.).

5.3.2 Circulation and Water Masses

The hydrography of shallow, intermediate, and deep waters in the Iceland Basin and Iceland Faroe Ridge are documented in multiple studies. One study found that warm and salty water originating from the Gulf Stream flows into the Norwegian Sea in the

upper layers above the Iceland-Faroe Ridge (Swift & Aagard, 1981). Part of the return flow takes place at deeper levels through the Faroe Channel bank and the Iceland-Faroe Ridge into the Iceland basin (van Aken & Eisma, 1987). A hydrographic study found that overflow waters from the Norwegian Sea mix with Sub-Polar Mode Water at the Iceland-Faroe Ridge, and Faroe Bank channel before descending into the deep Icelandic Basin to form the Iceland-Scotland Overflow Water (van Aken & De Boer, 1995). The process of formation of Iceland-Scotland Overflow water is depicted in Figure 5. It is important to document the hydrography and environmental characteristics of the study region because it gives insight into the factors that are controlling sea surface temperature, such as changes in incoming solar radiation, atmospheric oscillations, the meridional overturning circulation, and the greenhouse effect.

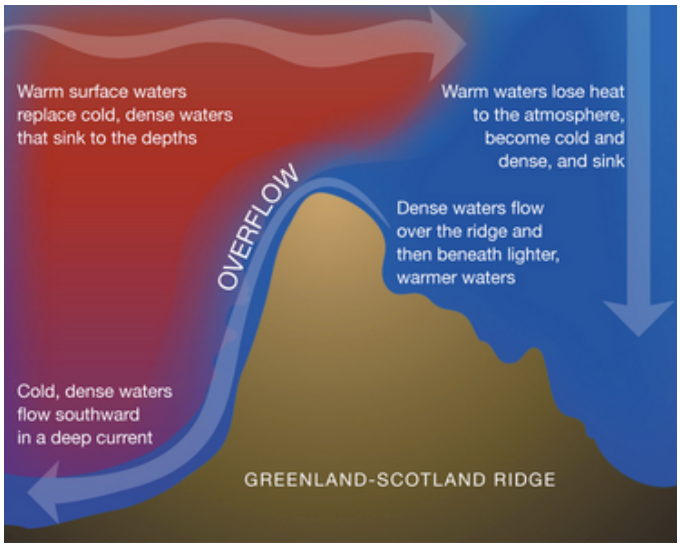

Figure 5. Formation of overflow waters over the Greenland-Scotland Ridge (Lipsett, 2012). The Iceland-Faroe Ridge is one section of the ridge depicted in this figure. The general process shown here is the mechanism for which the Iceland-Scotland Overflow Waters Form.

5.3.3 Environmental Characteristics

The environmental characteristics of the surface waters above the Iceland Basin and Iceland Faroe Ridge have been documented through the World Ocean Atlas 2013. The surface water measurements were taken at 0 m depth. Data from this atlas indicate that the average annual surface temperature, salinity, and dissolved oxygen content of this region are approximately 9°C, 35 psu, and 6.5 mL/L respectively (Locarnini et al., 2013; Zweng et al., 2013; Garcia et al., 2013). The environment of this region is relatively cold and salty with high levels of dissolved oxygen.

5.4 Icelandic Volcanism

The volcanism of Iceland is diverse and unique for an oceanic island because it has nearly every type of volcano and eruption style known on earth (Thordarsen & Larsen, 2007). The types of volcanoes range from archetypal mafic lava shields, to classical conal-shaped stratovolcanoes. The collective volcanic regions cover over 1/3 of Iceland, as shown in Figure 6 (Thordarsen & Larsen, 2007). The historical record contains 16 volcanic systems that were volcanically active over the last 1100 years. These systems were made up of 205 eruptive events that produced approximately 122 km^3 of tephra and lava (Thordarsen & Larsen, 2007).

Icelandic volcanoes have very sulphur-rich, explosive eruptions with the potential for great impacts on climate (Zielinski, 2000). High latitude eruptions are likely to cool only the climate in the hemisphere of origin because there is no significant interhemispheric transport of aerosols. The effect of these volcanic eruptions on the sea surface conditions of the Iceland basin requires further research.

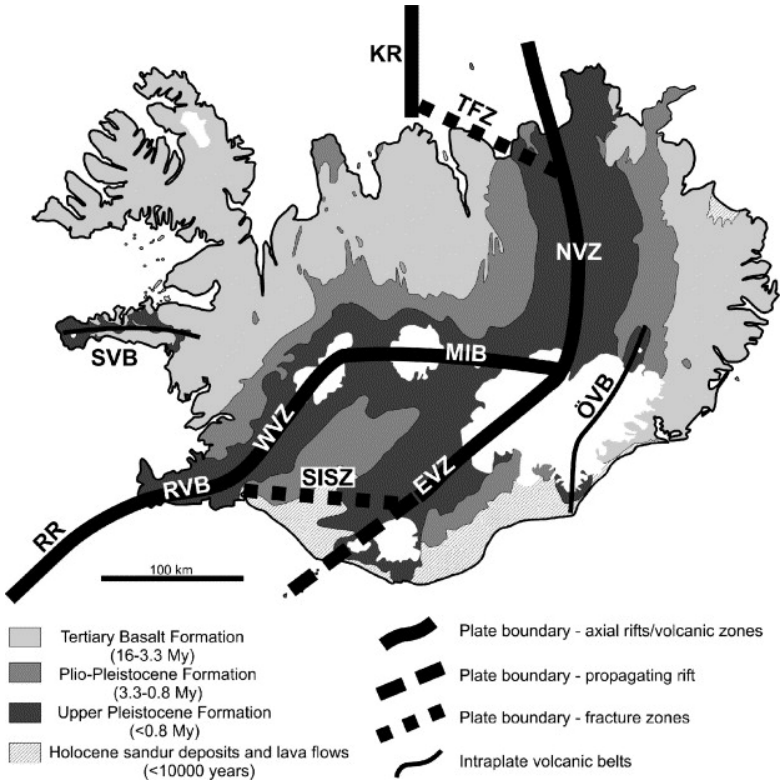

Figure 6. Schematic of the major fault structures, volcanic zones, and belts of Iceland. The abbreviations stand for: RR, Reykjanes Ridge; RVB, Reykjanes Volcanic Belt; SISZ, South Iceland Seismic Zone; WVZ, West Volcanic Zone; MIB, Mid-Iceland Belt; EVZ, East Volcanic Zone; NVZ, North Volcanic Zone; TFZ, Tjörnes Fracture Zone; KR, Kolbeinsey Ridge; ÖVB, Öræfi Volcanic Belt; SVB, Snæfellsnes Volcanic Belt (Thordarsen & Larsen, 2007).

5.5 Paleoreconstructions in the northern North Atlantic Ocean

5.5.1 Holocene SST reconstructions in the northern North Atlantic and Nordic Seas

The Holocene epoch is the most recent epoch in geologic time, dating from 0 to 11,700 years before present. The general trend of global annual SST in the Holocene shows Early Holocene warmth followed by a cooling trend through the Middle to Late Holocene (Marcott et al., 2013). Recent studies have made efforts to develop a high resolution SST record of the northern North Atlantic Ocean from this epoch.

A study by Sicre et al. (2008) reconstructed SST's over the last 4500 years north of Iceland from alkenones. The average temporal resolution of this Late Holocene record is between 2-5 years. The results of this study show that temperatures vary on bi- and multi-decadal timescales. The authors hypothesize that bidecadal oscillations are driven by the meridional overturning circulation (Sicre et al., 2008). The drivers of the larger amplitude multi-decadal SST oscillations are not as well understood, but are thought to be linked to the hydrological cycle of the tropical oceans and the NAO.

Large explosive volcanoes are also thought to have an influence on climatic conditions in the North Atlantic Ocean. Sicre et al. (2013) used alkenones and diatom IP_{25} proxy measures to reconstruct subdecadal variations of SST and sea ice in the subpolar North Atlantic caused by explosive tropical volcanic eruptions in the late thirteenth century. The results of the study showed short-term ocean cooling and sea ice expansion in response to each volcanic eruption. The longer-term effect, after volcanic forcing subsides, showed ice-free conditions and rapid warming of the surface ocean to values higher than pre-eruption, lasting several decades (Sicre et al., 2013). Sulfate

aerosols were likely the controlling factor on short-term cooling after the eruptions. The SST warming was likely triggered by sea-ice retreat and resumption of vertical mixing with deep waters (Sicre et al., 2013). Keeping these results in mind, it is reasonable to speculate that the climate would respond similar to volcanic eruptions originating from Iceland. Further research is needed to characterize the climatic effects of Icelandic volcanoes on the surrounding seas.

The northern North Atlantic SST reconstructions have focused on regions north of Iceland. Reconstructing Holocene SST from the Iceland Basin and Iceland-Faroe Ridge will provide further insight and confidence into our understanding of the Holocene climate variability.

5.5.2 SST Reconstruction in the Last Glacial Maximum

The Last Glacial Maximum (LGM) was the most recent point in time that glacial ice sheets were at a maximum extent. This event has been defined to extend from 19,000 to 23,000 years before present (Mix et al., 2001). There have been multiple, collaborative efforts to reconstruct sea surface conditions of the global ocean during the LGM. The first major project, namely the Climate Long-Range Investigation, Mapping and Prediction (CLIMAP) project, formed in the 1970s to study the history of global climate over the last million years. One of the goals of the project was to reconstruct the ocean's surface conditions at the LGM (CLIMAP Project Members, 1976). A surprising result of the reconstructions was that the sign and magnitude of surface temperature (SST) changes were significantly different between regions, as opposed to global unity (Mix et al, 2001). Results suggest that changes were greatest in the mid-to-high latitudes, especially the North Atlantic. These CLIMAP reconstructions are currently used to

evaluate GCM performance. Despite the revolutionary findings of the project, some of the results have recently been questioned.

The MARGO project (Multiproxy Approach for the Reconstruction of the Glacial Ocean surface) was launched in 2002 to provide a synthesis of all available proxy data and place them into a common framework to establish a multi-proxy global reconstruction of the LGM (Kucera et al., 2004). SSTs were estimated using multiple proxies including foraminiferal Mg/Ca ratios, foraminiferal oxygen isotope data and counts of assemblages of planktonic foraminifera, diatoms, radiolarian, and dinoflagellate cysts. The results indicate the strongest annual mean cooling (-10°C) to occur in the mid-latitude North Atlantic, as originally suggested by CLIMAP (MARGO Project Members, 2009). In contrast to CLIMAP, the MARGO data found that cooling was more pronounced in the eastern than in the western basin. It was also found that Mg/Ca based temperature reconstructions of tropical seas were estimated to be 2.0-3.5°C cooler than the present (Barker et al. 2005). This result is more in tune with climate model predictions of 2.5°C tropical cooling in the LGM (Crowley, 2000).

Complications arise in the MARGO reconstructions when analyzing the proxy estimates from high latitude cores. The results seem to be conflicting amongst different proxies. The Mg/Ca reconstructions suggest that no temperature differences exist between the Late Holocene and LGM at 60°N (Barker and Elderfield, 2002). Alkenone-based SST reconstructions, on the other hand, suggest that the Nordic Seas in the LGM were warmer than present values (Rosell-Melé and Comes, 1999), however the authors suggest there is likely a bias in the temperature signal. These biases are discussed in the next chapter, Section 6.6. A study using Mg/Ca reconstructions also shows

unrealistically warm temperatures in the central Nordic Seas (Meland et al., 2005). These authors hypothesize that the high Mg/Ca ratios could be due to significantly high salinities, resulting from salt rejection under sea-ice. Mg/Ca reconstructions of the southern part of the Nordic Seas are consistent with $\delta^{18}O$ reconstructions that suggest 0.5°C colder temperatures (Barker et al., 2005). The discrepancies in the high latitude results emphasize the need for more LGM SST reconstructions in this region.

5.6 Knowledge Gaps and Conclusions

The literature reviewed above shows that, even though there have been multiple studies that attempt to reconstruct SST in the northern North Atlantic Ocean and Nordic Seas, there are still uncertainties on the state of past sea surface climates at high latitudes. Attempts to reconstruct SST evolution of the Holocene have been focused around marine cores north of Iceland. There is a need for further Holocene climate research in the Iceland Basin and Iceland-Faroe Ridge. The results of LGM SST reconstructions demonstrate high uncertainty and conflicting results at high latitudes. The Iceland Basin, located at slightly lower latitudes than previous reconstructions, would be a good place to conduct further research because there is a higher chance of ice-free conditions during the LGM. The effect that Icelandic volcanism has on the surrounding sea surface conditions is still unknown, therefore requiring investigation.

In conclusion, there are no studies that have been done to reconstruct paleotemperatures in the Iceland Basin and Iceland-Faroe Ridge. Using alkenones to reconstruct SST dating back to the last glacial period is completely novel in this study region. The information gained from conducting research on the sea surface temperature of this region would help address the knowledge gaps identified in this literature review.

6.0 Methods

6.1 Overview

This chapter will outline the methods necessary to go about answering my research questions. I will first present the techniques that were used to collect sediment core 909-2 GC and the eleven core tops, during cruise POS457 by the R/V Poseidon. The route taken by this cruise is presented in Figure 2 of Section 4.3. I will then describe the details of the well-established laboratory procedure for analyzing alkenone unsaturation ratios, outlined in Kienast et al. (2006). A summary of data analysis techniques will then be given to describe how conclusions were drawn from my results. The reliability and uncertainty of using alkenone paleothermometry at high latitudes will be discussed in detail using results from previous literature.

6.2 Core Sampling

Core 909-2 GC originates from 62°50.20‘ N and 12°59.47‘ W at a depth of 755 m. The core was collected using a gravity corer with core barrel length of 10 m, and diameter 12.5 cm (GEOMAR Report, 2013). Once the core was hauled on ship, it was cut into 1 m sections and split into working and archive halves. The light reflectance of the sediment was measured using a hand-held Konica Minolta CM 600d spectrophotometer immediately after the core was split (GEOMAR Report, 2013). Archive halves were packaged in plastic tubes and stored at ~4°C.

Sampling of the core was executed using a non-probabilistic, systematic sampling method. This involved taking a 5 mL sample at every 10 cm, beginning at 0 cm. This method of sampling was chosen to get as equal an age distribution throughout the core, as possible.

The name, locations, and depths of the core tops collected are presented in Table 1. These core tops were collected using a 1.5-ton giant box corer, which is capable of collecting an undisturbed sediment body of 60 x 60 x 60 cm. The box corer was hauled on ship by the same mechanism as the gravity corer, and stored at ~4°C (GEOMAR Report, 2013). Once back in the lab, 5 mL samples were randomly extracted from each sediment body.

Table 1: This table presents the name, location, and depth of each of the core top samples collected and analyzed from cruise POS457.

Core Name	Latitude	Longitude	Depth (m)
GKG886-3	64°15.28‘	24°8.41‘	258
GKG888-1	63°17.50‘	23°33.99	323
GKG889-2	63°3.04‘	23°23.18‘	922
GKG899-3	63°20.44‘	17°56.78‘	157
GKG901-1	63°1.61‘	17°29.27‘	1292
GKG905-3	62°41.13‘	14°21.09‘	1610
GKG908-1	63°25.18‘	11°39.64‘	411
GKG909-1	62°50.28‘	12°59.56‘	755
GKG912-1	64°11.85‘	12°58.44‘	165
GKG914-1	64°11.13‘	12°50.94‘	261
GKG916-1	65°7.54‘	12°9.94‘	245

6.3 Alkenone Extraction

The alkenone extraction process follows the procedure laid out by Kienast et al. (2006). The full step-by-step procedure is presented in Figure 8 of the Appendix (Section 11.0). For each sample, 2 g of dry sediment was weighed and injected with 50 μL of internal standard. The internal standard is a solvent produced in the lab that contains known concentrations of carbon molecules C_{19}, C_{36}, and C_{40}. The total lipids were extracted from the sediment with organic solvent (93:7 DCM:MeOH) using an Accelerated Solvent Extraction system by Dionex (ASE200). The total lipid extract was then evaporated and saponified in a 0.5M KOH solution for 2 hours at 80°C. The sample

was then purified using silica gel chromatography to isolate the desired compounds. After purification, the extract was prepared for injection into the gas chromatographer by filling with 50 μL of hexane. The alkenones were then quantified through gas chromatography, which separates alkenones from the lipid extract based on their boiling points. Each of the three alkenones was represented on the chromatograph by a peak. The area under each peak represented the concentration of each alkenone in the sample.

The sea surface temperatures were then determined using the *Simplified Ketone Unsaturation Index* ($U^{k'}_{37}$), which calculates the ratio of the concentration of di-unsaturated and tri-unsaturated alkenones (See Equation 2 in Section 4.1). The SST corresponding to this index was calculated using the global core top calibration equation constructed by Müller et al. (1988): $SST\ (°C) = (U^{k'}_{37} - 0.044)/0.033$. This global calibration was chosen because it is the most widely used for alkenone paleothermometry. The core top $U^{k'}_{37}$ values were plotted against present day annual SST values of their respective location, and then compared to a global data set that follows Muller et al.'s calibration equation. This plot was used to check how well this region fits with the global calibration equation.

6.4 Data Analysis

In order to analyze the results, data were displayed in a plot of $U^{k'}_{37}$ versus core depth and SST versus core depth, using Microsoft Excel. The next step was to convert the depth values to the equivalent age of the core. This conversion was performed using an age model. The age model is usually developed through the use of two techniques: radiocarbon dating and ash layer dating. Radiocarbon dating uses the radioactive decay rate of Carbon-14 (^{14}C) to infer the amount of time passed since the organisms buried in

the sediment cores were alive. Living organisms take up the same ratio of ^{14}C as the atmosphere, which then decreases at a constant rate upon death. The ratio of ^{14}C to total carbon in a sample can be measured using accelerated mass spectrometry (Hughen, 2007). Ash layer dating uses the concept of tephrochronology to date ash layers in the core to known volcanic eruptions. The results of these two methods are combined to give absolute age points throughout the core. Average sedimentation rates are assumed between each point to infer a constant passing of time.

Unfortunately radiocarbon and ash layer dating were not completed by the time of writing this honours thesis. Instead, other age models had to be used to infer the relative age of the core. The first attempt at constructing an age model was through the preliminary age model based on lightness data of the sediment core.

The preliminary age model for core 909-2 GC is presented in Figure 7. This age model was determined by measuring light reflectance of the core after opening on board. The b* value reflects the ratio of blue and yellow colours in the sediment, which is indicative of biogenic silica production in this particular environment. Tentative results show that the core extends back approximately 120,000 years B.P. (GEOMAR report, 2013). The reliability of this age model will be discussed further in Section 8.1.

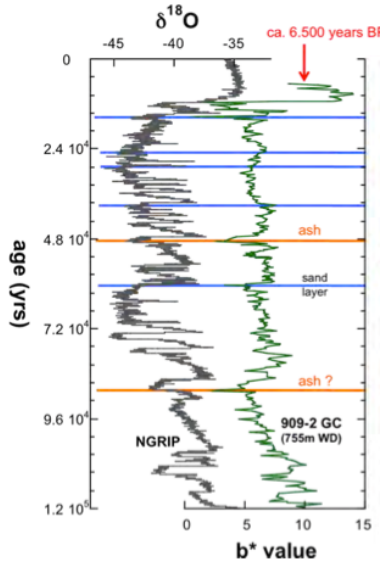

Figure 7. Preliminary age model of core 909-2 GC. The b* record of core 909-2 GC was plotted against the oxygen isotope stratigraphy of the North Greenland Ice Core Project (NGRIP) reference record. Orange and blue lines denote potential ash and sand layers respectively (GEOMAR Report, 2013).

After generating the data and plotting them as SST vs. age, error bars were added to the graph to account for uncertainties. Error ranges were determined based on analytical uncertainties and temperature uncertainties of the alkenone calibration. The calibration by Müller et al. (1998) has a standard error of estimate of ±1.5°C, which encompasses both the analytical uncertainty and calibration error. After the error bars were added to the graph, the data could be analyzed to look for variations through time. The error in age conversion could not be quantified because the absolute age model has not been completed.

Recall my hypothesis that sea surface temperatures over the Iceland-Faroe Ridge have been influenced by volcanic activity and changes in solar insolation. To test this hypothesis, I planned to determine the most likely causes of any temperature variations in

the results by comparing my findings with previous literature on this topic. I also planned to compare any temperature variations to known past volcanic events, and investigate whether a relationship exists.

6.5 Delimitations and Limitations

This study has been delimited temporally to a 10 cm resolution of the core. This means that there are only SST results from every 10 cm down the core, which could equate to an approximate 100-1000 year age gap between each data point. With this temporal resolution, I was not able to resolve SST variations that occur over relatively short time periods. A second delimitation was that only one SST proxy measure could be used within the scope of this thesis. Using multiple proxy measures reduces the amount of uncertainty in SST results.

The study is limited by the amount of alkenones present in the core and any uncertainties associated with alkenone reconstruction at high latitudes. These uncertainties are discussed in Section 6.6. There is also a large limitation involved with not having access to an absolute age model. This makes it difficult to draw many conclusions with confidence regarding the time frame of past climate variability.

6.6 Review of Alkenone Reliability and Uncertainties

Alkenone temperature signals are a good predictor of averaged annual SST, but there is a possibility of some seasonal bias based on the time of year that alkenone producing organisms were most abundant. Studies conducted in western North Atlantic surface waters found alkenone concentrations to be higher in the late winter and spring than other times of the year (Conte et al., 2001; Haidar & Thierstein, 2001) Another North Atlantic core top calibration found the strongest correlation between $U^{k'}_{37}$ and SST

in the autumn and winter months, but the correlation coefficient using annually averaged SSTs was still very high (Rosell-Melé et al., 1995). These seasonal biases will need to be taken into account when using alkenone temperature signals to reconstruct temperature patterns of the Iceland Basin.

Alkenone producing organisms live in the upper part of the water column in the euphotic zone and increase in abundance after storms. One study found that alkenone abundance is two to four times higher in the surface mixed layer (0-20 m) than in the deep fluorescent maximum (75-110 m) (Conte et al., 2001). Another study found alkenone-producing organisms to be most abundant in the upper 50 m of the water column where light is available (Haidar & Thierstein, 2001). Peak alkenone concentrations seem to be associated with storms that pass through the area, which is likely the time with highest nutrient availability (Conte et al., 2001). These studies demonstrate that alkenones are a fairly reliable indicator of temperature at the sea surface in the North Atlantic Ocean.

The $U^{k'}_{37}$ temperature calibration is limited at the extremes of *E. huxleyi's* growth temperature range. A study by Conte et al. (1998) found a reduction in the slope of the $U^{k'}_{37}$ calibration at temperatures <12°C and >21°C. A study published in 2004 found that $U^{k'}_{37}$ shows no correlation with sea surface temperatures below 8°C (Bendle & Rosell-Melé, 2004). Another study found that the use of the tetra-unsaturated alkenones in the U^{k}_{37} equation reduced the bias in temperature signals of cold waters in the Nordic Seas during the Last Glacial Maximum (LGM) (Rosell-Melé & Come, 1999). The waters of the Iceland Basin are relatively cold, therefore it may be useful to look at both $U^{k'}_{37}$ and U^{k}_{37} temperature calibrations, if tetra-unsaturated alkenones are present in the samples.

When analyzing the SST results from core 909-2-GC, it was important to consider the seasonality bias, abundance of *E. huxleyi* throughout the water column, and uncertainties in temperature calibrations that were outlined in this review. Although this study uses alkenones to reconstruct SST, it is recommended that future studies compare the results of another SST proxy to the findings of this thesis. The use of a second proxy would decrease the uncertainty in the results.

7.0 Results

7.1 Global Calibration Data

In order to determine how well the study region fits with the global ocean calibration, core top results from this study were compared to a set of global data. The resulting $U^{k'}_{37}$ values of the Iceland core tops were plotted against annually averaged temperature data from the World Ocean Atlas 2013. These data were plotted with a global data set compiled by Conte et al. (2006) to determine how well the Iceland data correlate with global core tops. The Müller et al. (1998) calibration equation was plotted through the data set with an error margin of 1.5°C. These results are presented in Figure 8. There appears to be a relatively strong fit with the global data set.

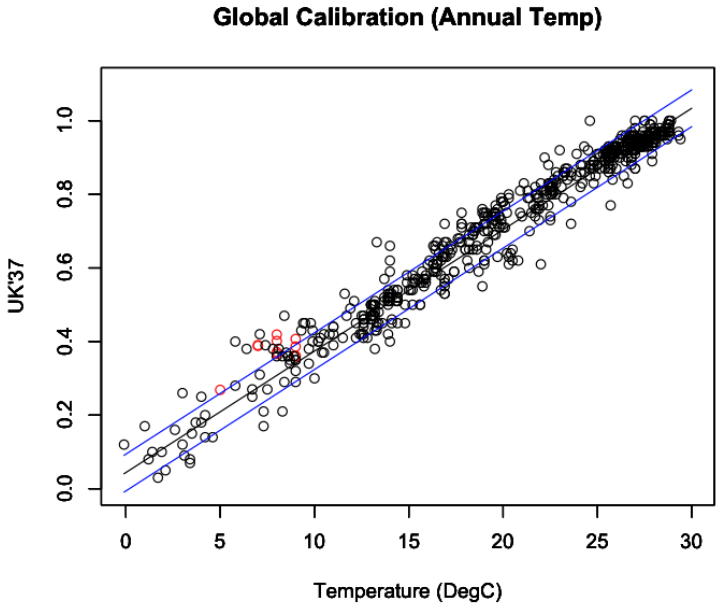

Figure 8. Plot of the resulting $U^{k'}_{37}$ vs. SST data from the Iceland core tops (red dots), plotted with a set of global coretop data (black dots) compiled by Conte et al. (2006). The blue lines show the 1.5°C uncertainty in the global calibration equation, which is $U^{k'}_{37}$=0.33*SST+0.044 (Müller et al., 1998).

7.2 Downcore Record of Uk'37 and SST

The resulting $U^{k'}_{37}$ data from the alkenone analysis on core 909-2 GC are presented in Figure 9. These data were plotted along the depth of the core. Initial results show two distinct warm periods in the past that peak at 30 and 600 cm, as well as a longer colder period between 200-500 cm.

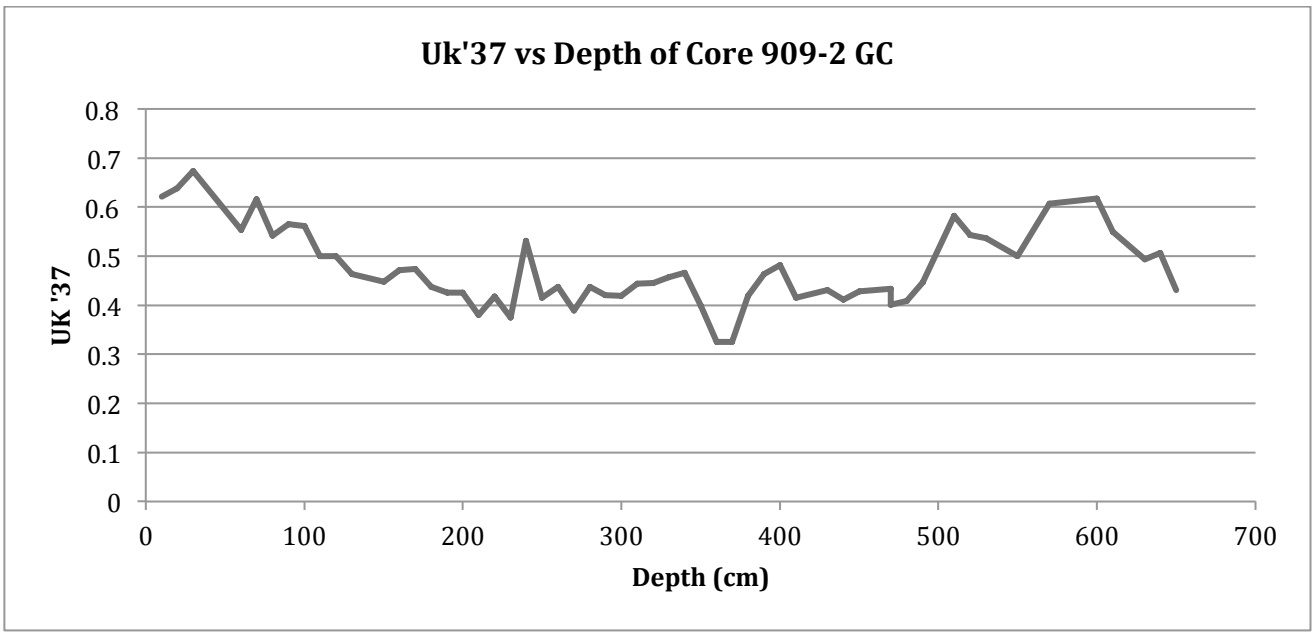

Figure 9. Plot of the $U^{k'}_{37}$ results along the depth of core 909-2 GC.

Since the core top data correlates well with the $U^{k'}_{37}$-SST calibration from global core top locations (as shown in Figure 8), the Müller et al. equation can be applied to 909-2 GC. The resulting SST data were plotted against the depth of the core in Figure 10. The error in this conversion is ±1.5°C, which is displayed with error bars along the y-axis. Temperature maxima of 19°C and 17°C are seen at 30 and 600 cm respectively, while the minimum temperature of 8.5°C is at 360 cm. It is evident that there is approximately a 9.5±1.5°C SST amplitude between the cold and warm periods.

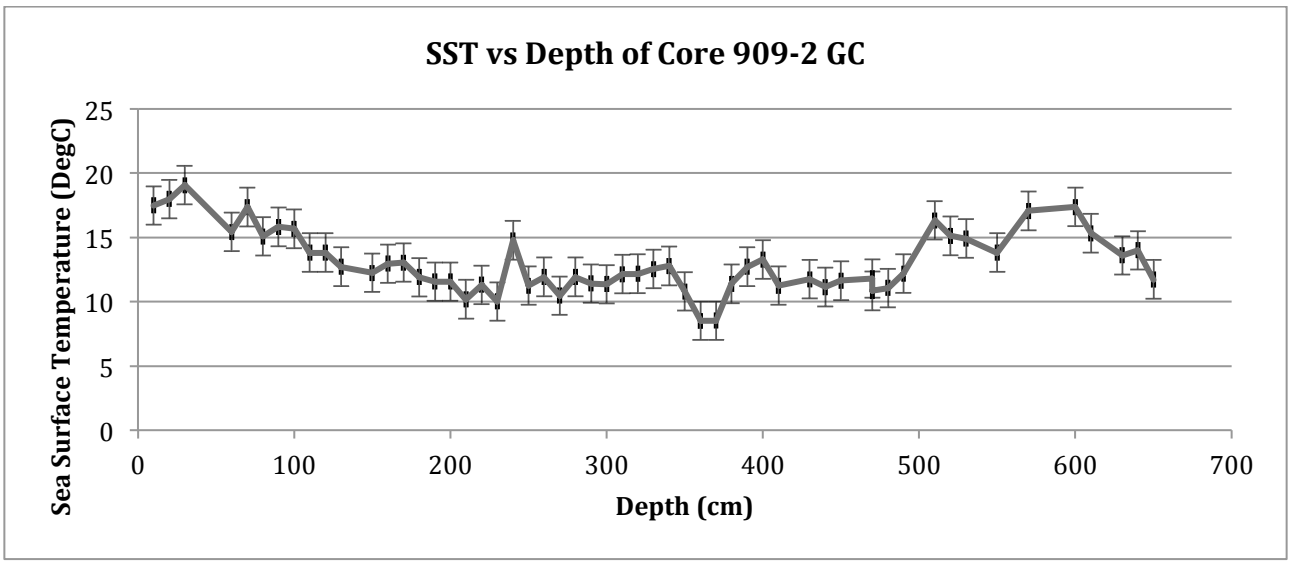

Figure 10. Plot of the SST values along the depth of core 909-2 GC. Error bars of ±1.5°C are displayed along the y-axis.

8.0 Discussion

8.1 Applying the Preliminary Age Model to Core 909-2 GC

The preliminary age model that was used to convert depth to age is presented in Figure 11. This age model was derived using b* data to align the depth of core 909-2 GC with the North Greenland Ice Core Project (NGRIP) $\delta^{18}O$ record (GEOMAR Report, 2013). $\delta^{18}O$ is a proxy measure for global ice volume, in which higher values indicate low ice volume, and lower values indicate high ice volume. This model was applied to Core 909-2 GC to generate the SST vs. age plot in Figure 12. The core top data point from giant box core 909-1 is also plotted with the downcore for comparison.

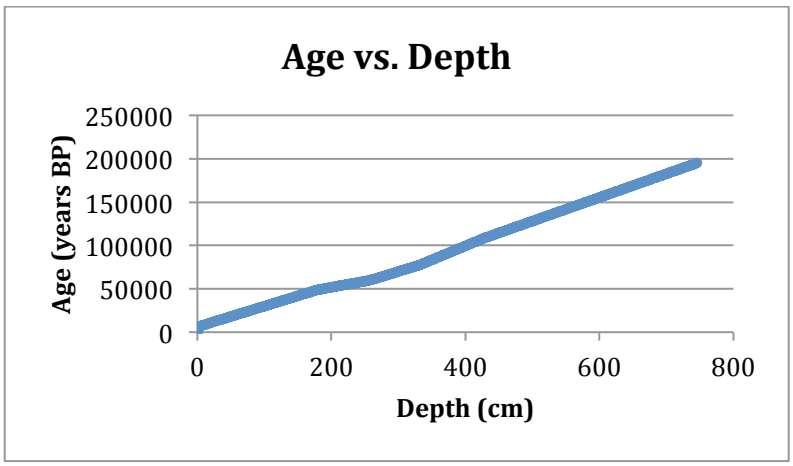

Figure 11. Plot of the preliminary age model used to convert the depth of core POS457-909-2 to age values. The age model uses the b* data and $\delta^{18}O$ of the NGRIP reference record initially presented in Figure 7.

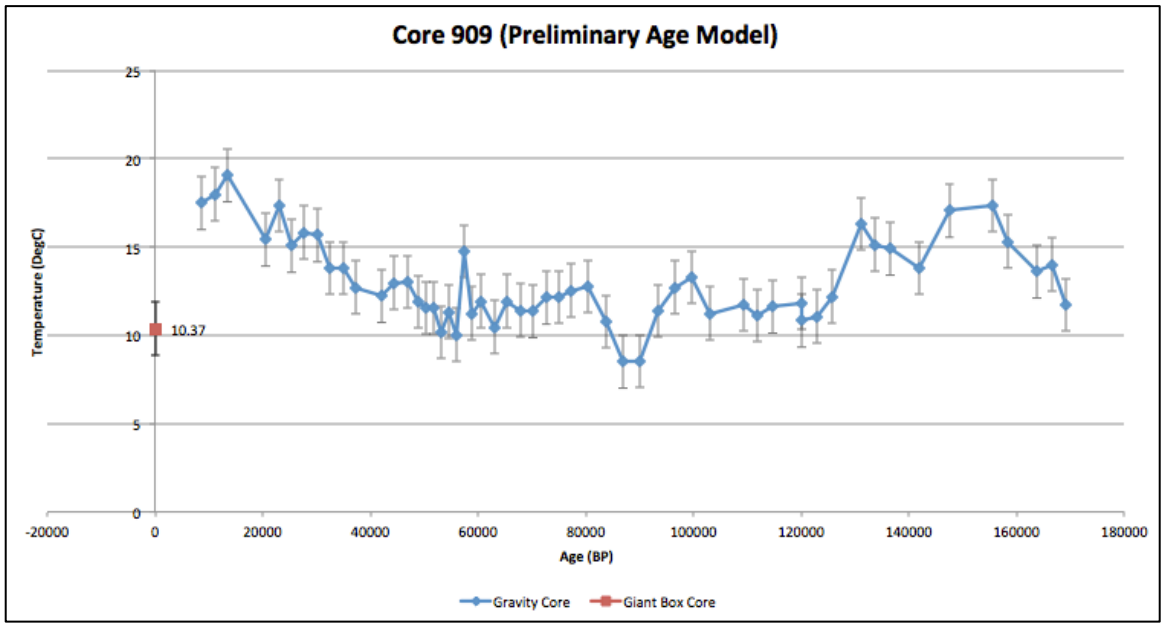

Figure 12. Plot of the SST vs. age record of Core 909-2 GC displayed with 1.5°C error bars. The data spans from 166700 to 8700 years before present (BP). The core top SST value from giant box core 909-1 is displayed at 0 years BP.

The general trends in Figure 12 show a warm period between 170,000 and 130,000 years BP, followed by a colder period from 120,000 to 30,000 years BP. SST increases from 30,000 years BP to 10,000 years BP, at which point it begins to cool towards present day values. The impression received after looking at the episodic trend in the data is that the core extends through two interglacial periods and one glacial period. The ages inferred from the preliminary age model do not seem to match up well with the established ages for these glacial cycle SST trends.

The Eemian was the most recent interglacial, spanning from 130,000 to 115,000 years BP. Based on the SST vs. age results in Figure 12 the Eemian would have been a period of relatively cold SST, which does not coincide with an expected interglacial SST trend. Looking at the general trend of Figure 10, it appears that the interglacial most likely occurred from 640-500 cm depth of the core. This could indicate that the preliminary age model is inaccurate for the deeper portion of the sediment core. Although it is impossible to clarify the age of the core without obtaining absolute age points, there are mechanisms for manipulating the data so that it makes more sense for interpreting. Section 8.2 will present two alternative age models by aligning the SST trends with the Eemian interglacial and Marine Isotope Stage 3 (MIS3), as displayed in the NGRIP $\delta^{18}O$ record of Figure 13.

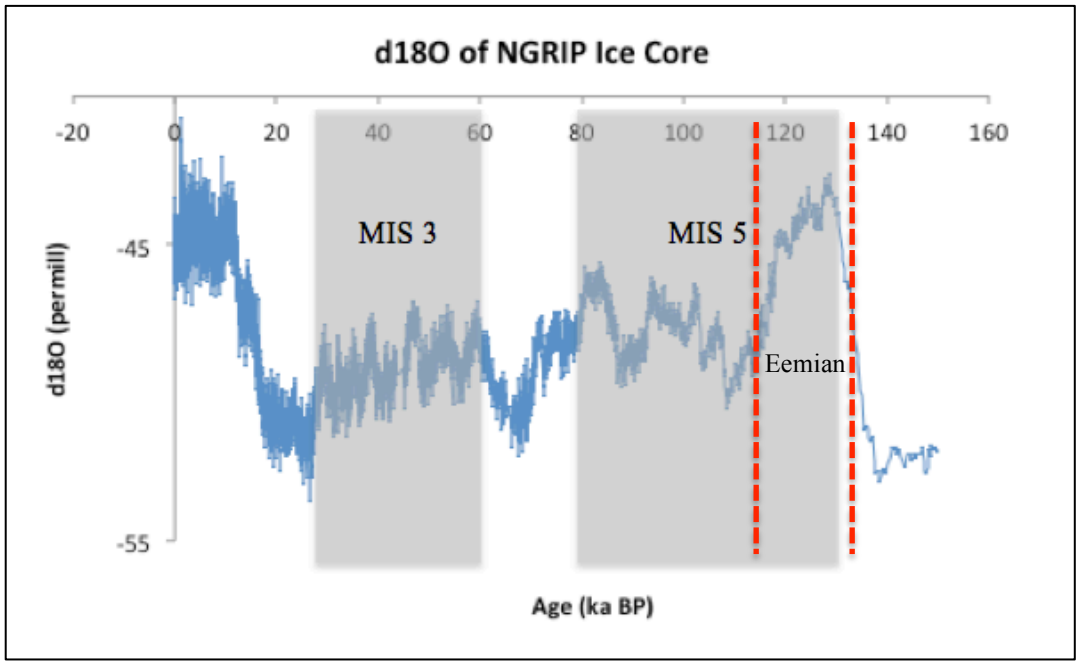

Figure 13. Plot of the NGRIP $\delta^{18}O$ record. Marine Isotopic Stage 3 (27-60 ka BP) and MIS 5 (80-130 ka) are highlighted in grey. Two red dashed lines note the Eemian interglacial.

8.2 Applying Age Models by aligning trends in $U^{k'}_{37}$ results with trends in the NGRIP Ice Core

8.2.1 Assuming Core 909-2 GC dates back to the Eemian interglacial period

The first reconstructed age model involves aligning $U^{k'}_{37}$ results with the NGRIP $\delta^{18}O$ record, under the assumption that POS457-909-2 extends back to the Eemian interglacial period. It essentially assigns age values to the points along the depth of the core, based on expected and well-understood trends in the data. These trends are assumed from previous climate reconstructions on other cores, like the NGRIP $\delta^{18}O$ record. This process was used on core 909-2 GC to construct a new SST vs. age plot that is dependent on the SST results. The new age model is presented in Figure 14, and the

resulting SST vs. age plot is presented in Figure 15. It is important to keep in mind that SST trends inferred from figure 15 do not have high confidence because the age is dependent upon the SST values. The final age model and associated uncertainties cannot be constructed until radiocarbon dating has been performed on the sediment core.

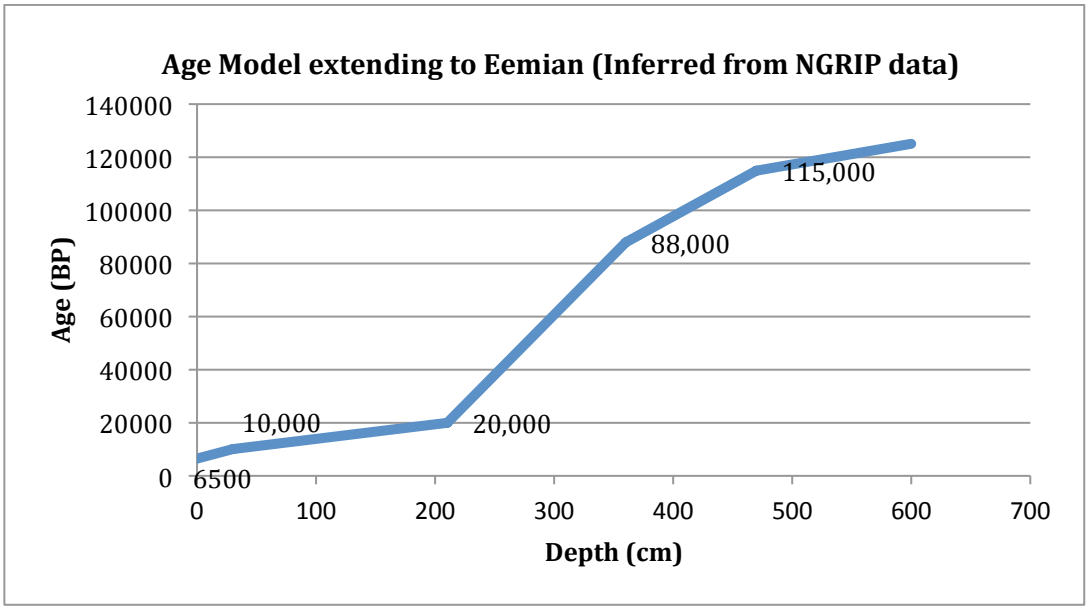

Figure 14. Plot of the age model inferred by matching arbitrary points from the SST results of core 909-2 GC with analogous points from the NGRIP $\delta^{18}O$ record, extending through the Eemian period. The slope of the line was linearly interpolated between each point.

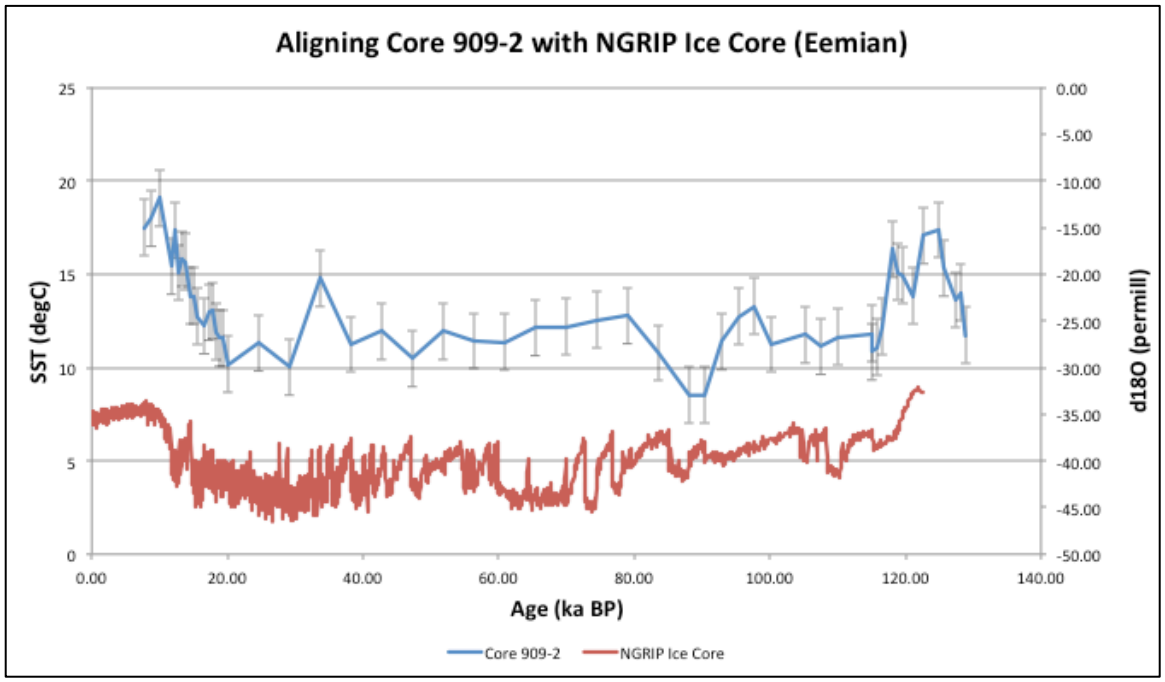

Figure 15. Plot of the SST vs. age plot after applying the age model from Figure 14. This plot is aligned with the $\delta^{18}O$ data from the NGRIP ice core. The SST values are displayed with 1.5°C error bars. This plot assumes that the core extends back through the Eemian interglacial period (115-130 kya).

Assuming that this age assignment is correct, we can conclude that the $U^{k'}_{37}$ paleothermometer portrays a warmer SST signal for the Holocene interglacial than the Eemian interglacial. This is an unanticipated result, as the literature shows a higher degree of warming in the Eemian compared to the Holocene (Leduc et al. 2010), due to the higher magnitude of solar insolation variance. The change in solar insolation on an interglacial to glacial timescale is a function of orbital configuration changes. The precession, obliquity and eccentricity of Earth's orbit around the sun determine the magnitude of solar insolation at a given point on the Earth (Müller, 2009). The Eemian was noted to be a period with high eccentricity, therefore the effects of precession on

insolation were pronounced, in comparison to the Holocene (Müller, 2009). This suggests that the age assignments of this age model are not strongly supported by previous literature. The following section will present a third age model that suggests the core only dates back into Marine Isotopic Stage 3.

8.2.2 Assuming Core 909-2 GC dates back to Marine Isotope Stage 3

This age model reconstruction involves aligning $U^{k'}_{37}$ results with the NGRIP $\delta^{18}O$ record, using the assumption that Core 909-2 GC extends back to Marine Isotope Stage 3 (60-30 kya BP). The similar peaks and distinct features were lined up between Core 909-2 and the NGRIP $\delta^{18}O$ record in order to construct the new age model, which is presented in Figure 16. The resulting SST vs. age plot is presented in Figure 17. As stated in Section 8.2.1, it is important to keep in mind that any conclusions drawn from Figure 17 have very high uncertainty because the assigned age is not independent of the SST results.

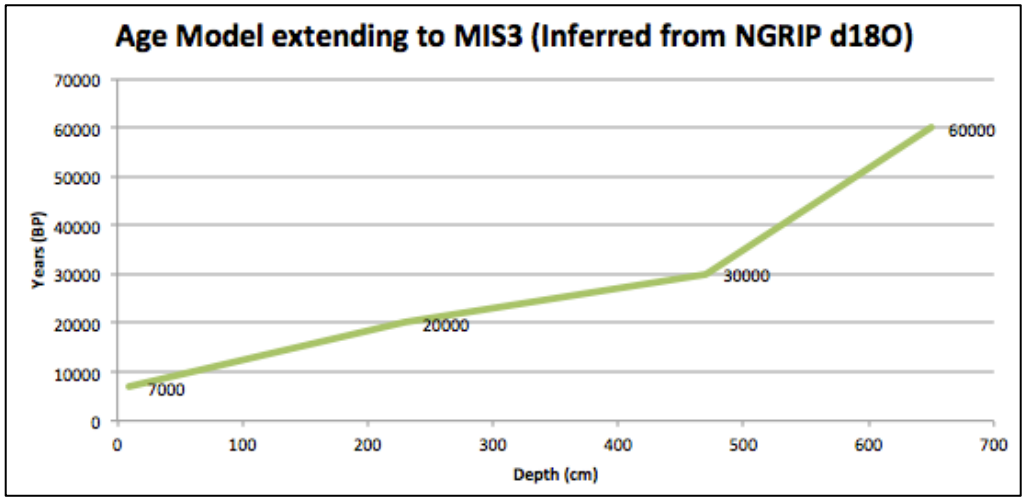

Figure 16. Plot of the age model inferred by matching arbitrary points from the SST results of core 909-2 with analogous points of the NGRIP ice core, extending to the start of MIS 3. The slope of the line was linearly interpolated between each point.

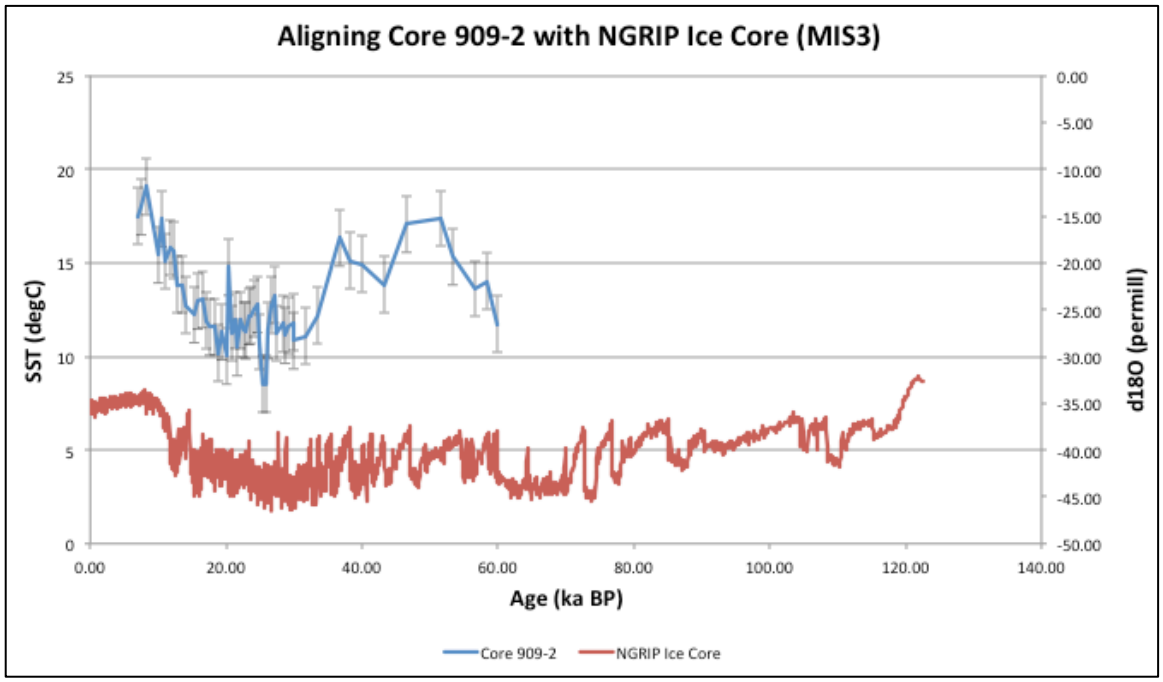

Figure 17. Plot of the SST vs. age plot after applying the age model from Figure 16. This plot is aligned with the $\delta^{18}O$ data from the NGRIP ice core. The SST values are displayed with 1.5°C error bars. This plot assumes that the core extends back to the onset of Marine Isotopic Stage 3 (60-30 kya).

Assuming that this age assignment is correct, we can conclude that the $U^{k'}_{37}$ paleothermometer portrays Marine Isotope Stage 3 to be almost as warm as the Holocene interglacial. Marine Isotope Stage 3 has been noted in the literature to experience many warm phases known as Dansgaard-Oeschger events (van Meerbeeck et al., 2009). These events are described by abrupt transitions from cold stadial conditions to warmer interstadial conditions (Dansgaard et al., 1993). The transitions between these conditions are likely driven by changes in the rate and location of NADW formation as a function of freshwater influx into the North Atlantic (Rahmstorf, 2002). The warm interstadial mode is likely associated with times of stronger Thermohaline Circulation (THC), while the cold stadial mode is associated with reduced THC (Rahmstorf, 2002). If MIS3 was

dominated by warm interstadial conditions, then there would have been increased heat transport to the northern North Atlantic. Under the assumption that this age model in Figure 16 is correct, the high SST values illustrated by Core 909-2 in MIS3 can be explained by this increased heat transport to the study site southeast of Iceland. Individual Daansgard-Oeschger events cannot be resolved because the temporal resolution of the core is too low.

8.3 Interpreting the Major Trends in Core POS457-909

8.3.1 Holocene Cooling

The results from all three age model reconstructions (Figures 12, 15, 17) indicate a cooling throughout the Holocene. For the purpose of this discussion, I will assume that the preliminary age model from Figure 11 is the correct age assignment to Core 909-2. Any SST and age values discussed throughout this section will come from the trends in Figure 12 of Section 8.1.

The cooling from the early Holocene to late Holocene is evident when comparing the SST results in the down core 909-2 to core top 909-1. A maximum SST value of 19.5±1.5°C is seen at 13,500 years BP, followed by a decline towards present day values of 10.4 ±1.5°C. These findings are supported by a study from Sachs et al. (2007), which reported 4-10 °C Holocene cooling in three North Atlantic cores using alkenone paleothermometry. The core locations are displayed in Figure 18. One suggested mechanism for this change was a decline in annual and summer insolation at mid-to-high latitudes, to similar levels of those from the LGM. This could cause the surface water cooling seen in the North Atlantic Ocean.

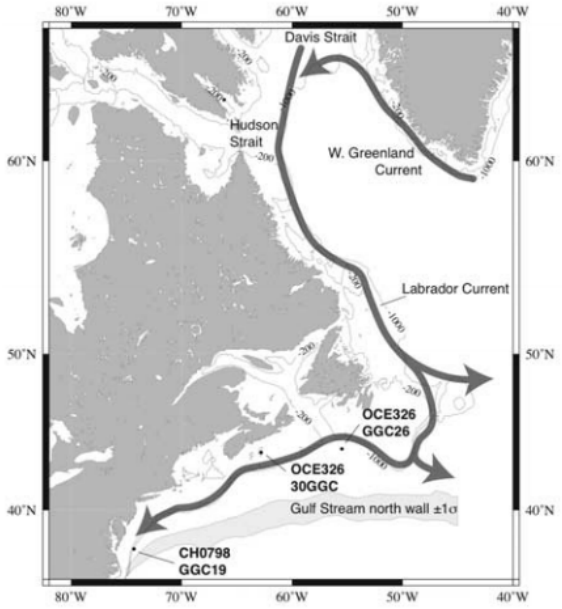

Figure 18. Locations of sediment cores analyzed in the Sachs et al. (2007) study. The surrounding ocean current locations are also included to indicate major water transport patterns in the proximity of the cores.

On the eastern side of the North Atlantic Ocean, the magnitude of cooling was only 1-3 °C (Marchal et al., 2002), suggesting a meridional gradient in the cooling trend across the North Atlantic (Sachs et al., 2007). Such a gradient could be explained by a negative phase in the North Atlantic Oscillation in the early Holocene, followed by a positive phase in the late Holocene. The positive phase may cause an increase in the intensity of westerly winds (Rennsen et al., 2005), which is thought to have increased the convection in the Labrador Sea (Marshall et al. 2001). This increased export of cold water via the Labrador Current could explain the substantial cooling in the cores from the western North Atlantic (Figure 13). Based on the location of core 909-2 GC over the Iceland-Faroe-Ridge (62°50.28' W 12°59.56'N), it is less likely that the increased strength of the Labrador Current would have a substantial effect on the Holocene cooling trend.

An alternative hypothesis suggested by Sachs et al (2007) was that there might have been a southward shift in the path of the Gulf Stream over the Holocene. This would have decreased the transport of warm equatorial water to the core sites in the Sachs et al. (2007) paper, hence explaining the Holocene cooling trend. The Iceland core site would feel this effect through the North Atlantic Current (NAC), which is a derivative of the Gulf Stream. It is possible that the NAC would have also shifted southward in response to the same forcing that moved the Gulf Stream.

8.3.2 Last Glacial Maximum

Another interesting result from the down core record of core 909-2 is that the SSTs from the LGM were significantly warmer than the present day SST value of core 909-1 (Figure 12). The core top value is 10.4 ±1.5°C, while the LGM values were around 15-17±1.5°C. This result is unexpected because the LGM is characterized as the point in the last glacial period with the maximum extent of glaciers, hence a very cold climate. These unrealistically warm LGM SSTs are supported by dinoflagellate cysts in the Nordic Seas, with absolute SST values of ~15°C (de Vernal et al., 2005). Other proxy measures, such as foraminiferal transfer functions, show much lower values around ~3-10°C (Sarnthein et al. 1995; Meland et al., 2005). These discrepancies may be explained by the presence of ice-rafted, Pre-Quaternary alkenones, or very high seasonal variation at high latitudes during the LGM.

Alkenone-derived SST values from a study in the Nordic Seas showed temperature values between 12 and 17°C (Rosell-Melé & Comes, 1999). The authors theorized that there might be a bias in the temperature signal during perennial ice cover because alkenone concentrations would be very low in the sediments. It would be

possible for a high amount of ice rafted debris contamination during this period, which could contain allochthonous alkenones with a warm pre-quaternary signal. Ice rafted alkenones would increase the autochthonous signal from $U^{k'}_{37}$=0.2 (~5°C) to 0.6 (~16°C) (Rosell-Melé & Comes, 1999). Despite ice-rafted debris being a plausible explanation for the warm SST signal, there is no evidence of ancient allochthonous alkenones in the sediment cores (Weaver et al., 1999; Rosell-Melé & Comes, 1999; de Vernal et al., 2006).

Another possible explanation for the warm temperature signals derived from alkenones could be the occurrence of high seasonality during the LGM. In a highly variable sea surface environment there would be seasonal ice-coverage, implying that alkenone production would only occur at the warmest part of the year. The resulting $U^{k'}_{37}$ imprint in sediments would reflect the summer SST rather than annual mean values (de Vernal et al., 2006). The summertime ice-free waters would be highly stratified, hence creating a large contrast between summer and winter SST (de Vernal et al., 2006).

Previous studies only found this discrepancy north of Iceland in the Nordic Seas. Results of this thesis suggest that this unusual LGM trend extends southeast of Iceland, above the Iceland-Faroe Ridge. Therefore these results support seasonal ice cover and high seasonality during the LGM.

If the other two age models of Section 8.2 are applied to the data, then we do not see any significant difference in SST between the LGM and core top data. This result will not be discussed because the age in these models was deliberately matched up to the depth that most resembled the LGM. This once again highlights the need to obtain

absolute dating of the core samples in order to have increased confidence in the past climate variability of the seas above the Iceland-Faroe-Ridge.

9.0 Conclusions

Regardless of the age model selected, there are two minimal conclusions that can be drawn from the results. Firstly, the Late Holocene represented in the giant box core top is significantly colder than the early Holocene from the top of the gravity core. Secondly, it is evident that there were two distinct past warm periods sampled by the core. The warm event between 500 and 650 cm was slightly cooler than the warm event of the early Holocene. Since there were no absolute age points determined during the time frame of this thesis, three potential age model scenarios were proposed.

When the preliminary age model from 8.1 was applied to the results, the alkenone derived SSTs of the LGM showed much warmer SSTs than present day values. This unanticipated result could be explained by the presence of ice-rafted, Pre-Quaternary alkenones, or very high seasonal variation at high latitudes during the LGM. The deeper portion of the core also resulted in unexpected trends. The earlier warm period does not align well with any known SST trends from this region. After speculation and comparison to previous literature, it was hypothesized that this warm period between 500 and 650 cm may be the Eemian interglacial period or Marine Isotope Stage 3. Using these hypotheses, two additional age models were constructed to illustrate different pictures of the past climate above the Iceland-Faroe-Ridge.

If it is assumed that the core dates back to the previous interglacial, then the data imply that the Eemian was slightly cooler than the Holocene interglacial. This is an unexpected result because the literature suggests stronger solar insolation in the Eemian

compared to the Holocene, hence warmer SSTs. If it is assumed that the core dates back to MIS 3, then we can conclude that MIS 3 was almost as warm as the Holocene. This result is better supported by the literature, as MIS 3 has been noted to be a period with a high frequency of Dansgaard-Oeshger events. A large frequency of these events would likely be associated with stronger thermohaline circulation and increased heat transport to the northern North Atlantic Ocean. This increased heat transport could explain the observed SSTs above the Iceland-Faroe-Ridge for this time period.

It is evident that the largest uncertainty and limitation in this study is assigning age values. In order to increase our confidence in the results, radiocarbon dating and ash layer dating should be performed on the core samples. These absolute age points should then be used to construct a more reliable age model to apply to Core 909-2.

In Section 4.3, I hypothesized that solar insolation and the volcanoes of Iceland have a significant influence on the SST variability of this region. Despite high uncertainty in the age assignment, I would conclude that the SST downcore record provides some evidence in support of solar insolation as a significant influence. The low temporal resolution of the core makes it difficult to resolve any effects of volcanic activity on the SST of this region, therefore I do not have sufficient evidence to reject my hypothesis. In addition to solar insolation and volcanic activity, I would also add that changes in global ocean circulation likely play a large role in determining the climatic conditions of the Iceland-Faroe-Ridge.

To increase our understanding of past climate variability in the regions southeast of Iceland, I suggest further research to reconstruct alkenone SSTs from additional sediment cores. It would also be useful to reconstruct SSTs using an alternative proxy

method, such as Mg/Ca ratios in planktonic foraminifera (Nürnberg, 1995). Using additional sediment cores and SST indicators will illustrate a better picture of the variations and controlling mechanisms of past climates in this region.

The significance of these results will be clearer after the completion of a reliable age model. Once the final ages are assigned, the SST data collected from this thesis will be added to a large data archive that can be accessed by other climate scientists. These data may be used in future review papers that synthesize existing SST data to help illustrate a global picture of the past ocean. These data may also be used by modelers to help test the reliability of general circulation models.

10.0 Bibliography

Bagley, M. (2013). Holocene epoch: The age of man. *LiveScience*. Retrieved from: http://www.livescience.com/28219-holocene-epoch.html

Barker, S., & Elderfield, H. (2002). Foraminiferal calcification response to glacial-interglacial changes in atmospheric CO2. *Science*, *297*(5582), 833-836.

Barker, S., Cacho, I., Benway, H., & Tachikawa, K. (2005). Planktonic foraminiferal Mg/Ca as a proxy for past oceanic temperatures: a methodological overview and data compilation for the Last Glacial Maximum. *Quaternary Science Reviews*, *24*(7), 821-834.

Bendle, J., & Rosell-Melé, A. (2004). Distributions of UK37 and UK37′ in the surface waters and sediments of the Nordic Seas: Implications for paleoceanography. *Geochemistry, Geophysics, Geosystems*, *5*(11).

Bindoff, N. L., Willebrand, J., Artale, V., Cazenave, A., Gregory, J. M., Gulev, S., ... & Unnikrishnan, A. S. (2007). Observations: oceanic climate change and sea level.

Bopp, L., Resplandy, L., Orr, J. C., Doney, S. C., Dunne, J. P., Gehlen, M., ... & Vichi, M. (2013). Multiple stressors of ocean ecosystems in the 21st century: projections with CMIP5 models. *Biogeosciences*, *10*(10), 6225-6245.

Brassel S. C., Eglinton G., Marlowe I. T., Pflaumann U., Sarnthein M. (1986) Molecular stratigraphy: A new tool for climatic assessment. *Nature.* 320, 129-133

Conte, M. H., Thompson, A., Lesley, D., & Harris, R. P. (1998). Genetic and Physiological Influences on the Alkenone/Alkenoate Versus Growth Temperature Relationship in Emiliania huxleyi and Gephyrocapsa Oceanica. *Geochimica et Cosmochimica Acta*, *62*(1), 51-68.

Conte, M. H., Weber, J. C., King, L. L., & Wakeham, S. G. (2001). The alkenone temperature signal in western North Atlantic surface waters. *Geochemica et Cosmochemica Acta.* 65(23), 4275-4287.

Conte, M. H., Sicre, M. A., Rühlemann, C., Weber, J. C., Schulte, S., Schulz‐Bull, D., & Blanz, T. (2006). Global temperature calibration of the alkenone unsaturation index (UK′ 37) in surface waters and comparison with surface sediments. *Geochemistry, Geophysics, Geosystems*, *7*(2).

CLIMAP, P. M. (1976). The surface of the ice-age earth. *Science (New York, NY)*, *191*(4232), 1131.

Dansgaard, W., Johnsen, S. J., Clausen, H. B., Dahl-Jensen, D., Gundestrup, N. S., Hammer, C. U., ... & Bond, G. (1993). Evidence for general instability of past climate from a 250-kyr ice-core record. *Nature*, *364*(6434), 218-220.

de Boisseson, E., Thierry, V., Mercier, H., & Caniaux, G. (2010). Mixed layer heat budget in the iceland basin from argo. *Journal of Geophysical Research, 115*. doi:http://dx.doi.org/10.1029/2010JC006283

de Vernal, A., Turon, J. L., & Guiot, J. (1994). Dinoflagellate cyst distribution in high-latitude marine environments and quantitative reconstruction of sea-surface salinity, temperature, and seasonality. *Canadian Journal of Earth Sciences*, *31*(1), 48-62.

de Vernal, A., Eynaud, F., Henry, M., Hillaire-Marcel, C., Londeix, L., Mangin, S., ... & Turon, J. L. (2005). Reconstruction of sea-surface conditions at middle to high latitudes of the Northern Hemisphere during the Last Glacial Maximum (LGM) based on dinoflagellate cyst assemblages. *Quaternary Science Reviews*,*24*(7), 897-924.

de Vernal, A., Rosell-Melé, A., Kucera, M., Hillaire-Marcel, C., Eynaud, F., Weinelt, M., . . . Kageyama, M. (2006). Comparing proxies for the reconstruction of LGM sea-surface conditions in the northern north atlantic. *Quaternary Science Reviews, 25*(21), 2820-2834.

Dekens, P. S., Ravelo, A. C., McCarthy, M. D., & Edwards, C. A. (2008). A 5 million year comparison of Mg/Ca and alkenone paleothermometers.*Geochemistry, Geophysics, Geosystems*, *9*(10).

Denmark Strait. (n.d.). Retrieved November 23, 2014, from http://oceana.org/en/explore/marine-places/denmark-strait

Eglinton, T. (2007) Follow the carbon trail. *Oceanus Magazine.* Retrieved from: http://www.whoi.edu/oceanus/feature/follow-the-carbon-trail

Garcia, H. E., Locarnini, R. A., Boyer, T. P., Antonov, J. I., Baranova, O.K., Zweng, M.M., Reagan, J.R., & Johnson, D.R. (2014). *World Ocean Atlas 2013, Volume 3: Dissolved Oxygen, Apparent Oxygen Utilization, and Oxygen Saturation.* S. Levitus, Ed., A. Mishonov Technical Ed.; NOAA Atlas NESDIS 75, 27 pp.

GEOMAR Report (August, 2013). Volcanic risks from iceland and climate change: The late quaternary to anthropogene development. *R/V Poseidon Cruise Report.* Fig 4.8. DOI: 10.3289/GEOMAR_REP_NS_14_2014

Haidar A.T. and Thierstein H.R. (2001) Coccolithophore dynamics off Bermuda (N. Atlantic). *Deep-Sea Research Pt. II*. 48, 1925–1956

Hald, M., Andersson, C., Ebbesen, H., Jansen, E., Klitgaard-Kristensen, D., Risebrobakken, B., ... & Telford, R. J. (2007). Variations in temperature and extent of Atlantic Water in the northern North Atlantic during the Holocene. *Quaternary Science Reviews*, *26*(25), 3423-3440.

Hughen, K. A. (2007). Radiocarbon dating of deep-sea sediments. *Developments in Marine Geology, A. eds*, 185-210.

Hughes, T. M., & Weaver, A. J. (1994). Multiple equilibria of an asymmetric two-basin ocean model. *Journal of Physical Oceanography*, *24*(3), 619-637.

Kienast, M., Kienast, S. S., Calvert, S. E., Eglinton, T. I., Mollenhauer, G., François, R., & Mix, A. C. (2006). Eastern Pacific cooling and Atlantic overturning circulation during the last deglaciation. *Nature*, *443*(7113), 846-849.

Kirk, J. T. O. (1994). *Light and Photosynthesis in Aquatic Ecosystems*. Cambridge University Press, New York.

Koc Karpuz, N., & Schrader, H. (1990). Surface sediment diatom distribution and Holocene paleotemperature variations in the Greenland, Iceland and Norwegian Sea. *Paleoceanography*, *5*(4), 557-580.

Kucera, M., Rosell-Melé, A., Schneider, R., Waelbroeck, C., & Weinelt, M. (2005). Multiproxy approach for the reconstruction of the glacial ocean surface (MARGO). *Quaternary Science Reviews*, *24*(7), 813-819.

Latif, M., Böning, C., Willebrand, J., Biastoch, A., Dengg, J., Keenlyside, N., ... & Madec, G. (2006). Is the thermohaline circulation changing?. *Journal of Climate*, *19*(18), 4631-4637.

Leduc, G., Schneider, R., Kim, J. H., & Lohmann, G. (2010). Holocene and Eemian sea surface temperature trends as revealed by alkenone and Mg/Ca paleothermometry. *Quaternary Science Reviews*, *29*(7), 989-1004.

Lipsett, L. (2012). A newfound cog in the ocean conveyor. *Oceanus Magazine*. Retrieved from: http://www.whoi.edu/oceanus/feature/a-newfound-cog-in-the-ocean-conveyor

Locarnini, R. A., Mishonov, A. V., Antonov, J. I., Boyer, T. P., Garcia, H. E., Baranova, O. K., Zweng, M. M., Paver, C. R., Reagan, J. R., Johnson, D. R., Hamilton, M., & Seidov, D. (2013). *World Ocean Atlas 2013, Volume 1: Temperature.* S. Levitus, Ed., A. Mishonov Technical Ed.; NOAA Atlas NESDIS 73, 40 pp.

Lowe, D. J. (2011). Tephrochronology and its application: a review. *Quaternary Geochronology*, *6*(2), 107-153.

Malmberg, S. A. (2004). The Iceland basin: topography and oceanographic features. Marine Research Institute. Report 109, 43 s.

Marchal, O., Cacho, I., Stocker, T. F., Grimalt, J. O., Calvo, E., Martrat, B., ... & Jansen, E. (2002). Apparent long-term cooling of the sea surface in the northeast Atlantic and Mediterranean during the Holocene. *Quaternary Science Reviews*, *21*(4), 455-483.

Marcott, S. A., Shakun, J. D., Clark, P. U., & Mix, A. C. (2013). A reconstruction of regional and global temperature for the past 11,300 years. *science*,*339*(6124), 1198-1201.

Marshall, J., Kushnir, Y., Battisti, D., Chang, P., Czaja, A., Dickson, R., ... & Visbeck, M. (2001). North Atlantic climate variability: phenomena, impacts and mechanisms. *International Journal of Climatology*, *21*(15), 1863-1898.

Meland, M. Y., Jansen, E., & Elderfield, H. (2005). Constraints on SST estimates for the northern North Atlantic/Nordic Seas during the LGM.*Quaternary Science Reviews*, *24*(7), 835-852.

Mix, A. C., Bard, E., & Schneider, R. (2001). Environmental processes of the ice age: land, oceans, glaciers (EPILOG). *Quaternary Science Reviews*, *20*(4), 627-657.

Müller, P. J., Kirst, G., Ruhland, G., von Storch, I., and Rosell-Mele, A. (1998) Calibration of the alkenone paleotemperature index $U^{k'}_{37}$ based on core-tops from the eastern South Atlantic and the global ocean (608N–608S). *Geochim.Cosmochim. Acta* 62, 1757–1772.

Müller, U. C. (2009). Eemian (Sangamonian) Interglacial. In *Encyclopedia of Paleoclimatology and Ancient Environments* (pp. 302-307). Springer Netherlands.

Nürnberg D. (1995) Magnesium in tests of Neogloboquadrina Pachyderma sinistral from high Northern and Southern latitudes. *J. Foraminiferal Res*. 25(4), 350–368.

Prahl F. G., Wakeham S. G. (1987) Calibration of unsaturation patterns in long-chain ketone compositions for paleotemperature assessment. *Nature.* 330, 367-369

Renssen, H., Goosse, H., Fichefet, T., Masson-Delmotte, V., & Koç, N. (2005). Holocene climate evolution in the high-latitude Southern Hemisphere simulated by a coupled atmosphere-sea ice-ocean-vegetation model. *The Holocene*,*15*(7), 951-964.

Rosell-Melé, A., Eglinton, G., Pflaumann, U., & Sarnthein, M. (1995). Atlantic core-top calibration of the U37K index as a sea-surface palaeotemperature indicator. *Geochimica et Cosmochimica Acta*,*59*(15), 3099-3107.

Rosell-Melé, A. (1998). Interhemispheric appraisal of the value of alkenone indices as temperature and salinity proxies in high-latitude locations. *Paleoceanography*, *13*(6), 694-703.

Rosell-Melé, A., & Comes, P. (1999). Evidence for a Warm Last Glacial Maximum in the Nordic Seas or an example of shortcomings in UK 37′ and UK 37 to estimate low sea surface temperature?. *Paleoceanography*, *14*(6), 770-776.

Sachs, J. P. (2007). Cooling of Northwest Atlantic slope waters during the Holocene. *Geophysical research letters*, *34*(3).

Saher, M. H., Rostek, F., Jung, S. J. A., Bard, E., Schneider, R. R., Greaves, M., ... & Kroon, D. (2009). Western Arabian Sea SST during the penultimate interglacial: A comparison of U37K′ and Mg/Ca paleothermometry. *Paleoceanography*, *24*(2).

Sarnthein, M., Winn, K., Jung, S. J., Duplessy, J. C., Labeyrie, L., Erlenkeuser, H., & Ganssen, G. (1994). Changes in east Atlantic deepwater circulation over the last 30,000 years: Eight time slice reconstructions. *Paleoceanography*, *9*(2), 209-267.

Sicre, M. A., Khodri, M., Mignot, J., Eriksson, J., Knudsen, K. L., Ezat, U., Closset, I., Nogues, P., & Massé, G. (2013). Sea surface temperature and sea ice variability in the subpolar North Atlantic from explosive volcanism of the late thirteenth century. *Geophysical Research Letters*. 40, 5536-5530 doi:10.1002/2013GL057282.

Sikes, E. L., Volkman. J. K., Robertson, L. G. & Pichon. J. J. (1997) Alkenones and alkenes in surface waters and sediments of the Southern Ocean: Implications for paleotemperature estimation in polar regions. Geochemica et Cosmochimica Acta. 61. 1495-1505

Sóron, A. S. (2009) A Garábi Slír Formáció foraminifera faunájának vizsgálata. MSc Thesis, Eötvös Loránd University. Plate 5, Fig. 8. Retrieved from http://foraminifera.eu/singlea.php?no=1002811&aktion=suche

Swift J. I. & Aargard, K (1981). Seasonal transitions and water mass formation in the Iceland and Greenland Seas. *Deep-Sea Research.* 28, 1107-1129.

Thordarson, T., & Larsen, G. (2007). Volcanism in Iceland in historical time: Volcano types, eruption styles and eruptive history. *Journal of Geodynamics*,*43*(1), 118-152.

van Aken, H. M. & Eisma, D. (1987). The circulation between Iceland and Scotland derived from water mass analysis. *Netherlands Journal of Sea Research*, 21, 1-15.

Van Meerbeeck, C. J., Renssen, H., & Roche, D. M. (2009). How did Marine Isotope Stage 3 and Last Glacial Maximum climates differ?–perspectives from equilibrium simulations. *Climate of the Past*, *5*(1), 33-51.

Weaver, P. P. E., Chapman, M. R., Eglinton, G., Zhao, M., Rutledge, D., & Read, G. (1999). Combined coccolith, foraminiferal, and biomarker reconstruction of

paleoceanographic conditions over the past 120 kyr in the northern North Atlantic (59 N, 23 W). *Paleoceanography*, *14*(3), 336-349.

Zielinski, G. A. (2000). Use of paleo-records in determining variability within the volcanism–climate system. *Quaternary Science Reviews*, *19*(1), 417-438.

Zweng, M.M, Reagan, J.R., Antonov, J.I., Locarnini, R.A., Mishonov, A.V., Boyer, T.P., Garcia, H.E., Baranova, O.K., Johnson, D.R., Seidov, D., & Biddle, M.M. (2013). *World Ocean Atlas 2013, Volume 2: Salinity.* S. Levitus, Ed., A. Mishonov Technical Ed.; NOAA Atlas NESDIS 74, 39 pp.

11.0 Appendix: Lab Procedure

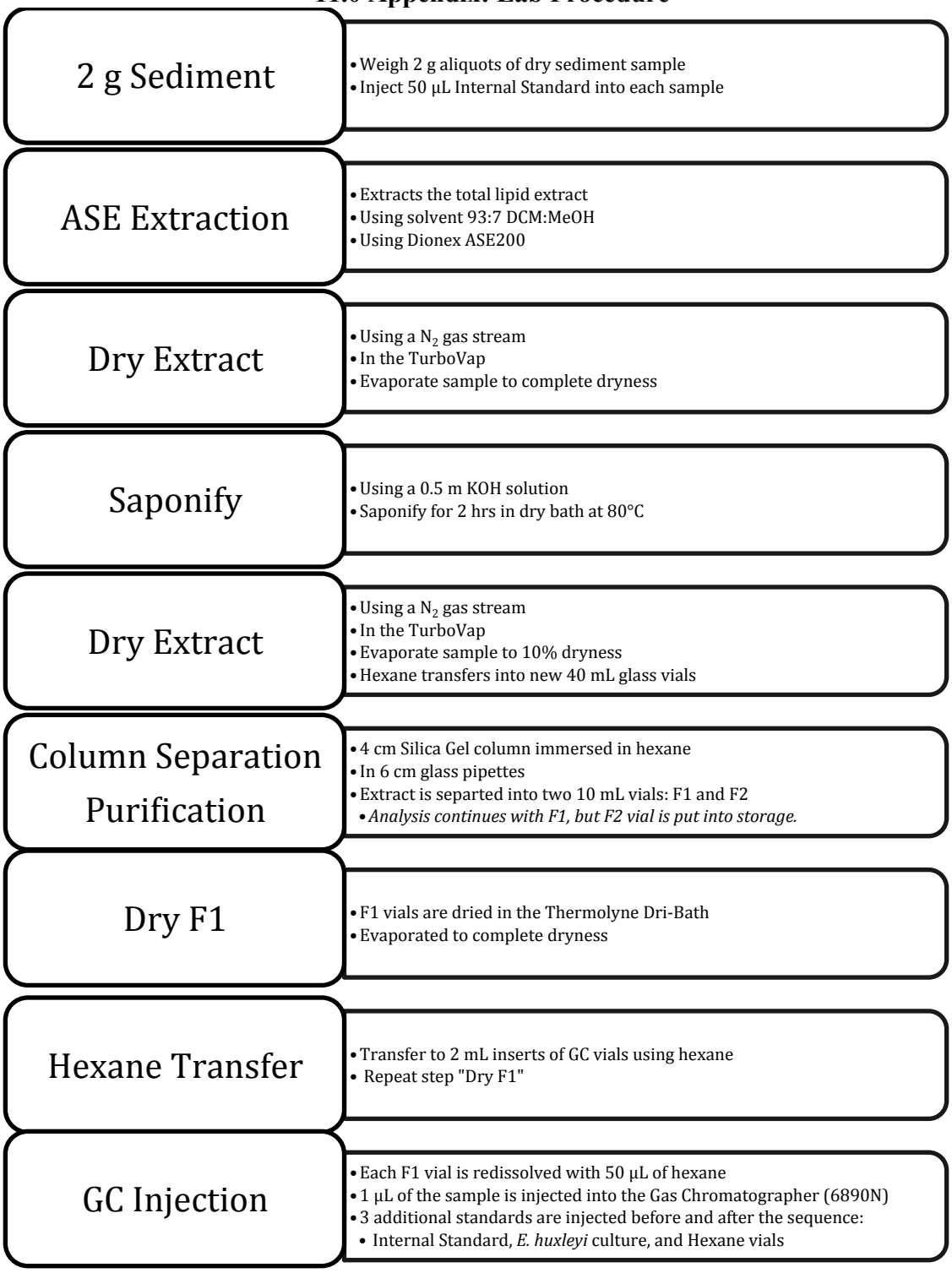

Figure 14. This figure presents a flow chart of the laboratory procedure used for alkenone analysis in the sedimentary geochemical lab at Dalhousie University. This method was established by Kienast et al. (2006).

12.0 Appendix: Gantt Chart

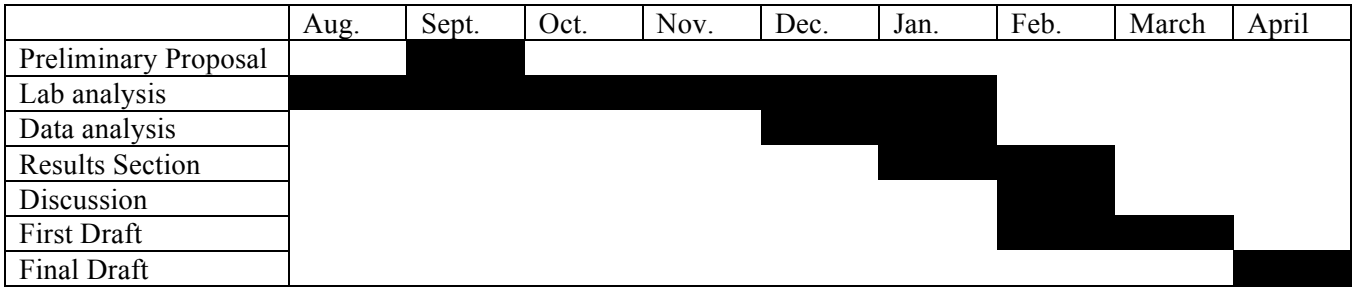

Figure 15. This figure presents the Gantt chart of the timelines set out for the components of my hounours thesis.